www.czasopisma.pan.pl PAN www.journals.pan.pl

INTL JOURNAL OF ELECTRONICS AND TELECOMMUNICATIONS, 2021, VOL. 67, NO. 4, PP. 579-587
Manuscript received May 10, 2020; revised November, 2021 DOI:10.24425/ijet.2021.137849

A Review on Impulse RADAR

Saket Kumar, Amit Kumar, Vikrant Singh, and Abhishek Kumar Singh

***Abstract*—RADAR plays a vital role in military applications since its origin in the 2nd world war. Recently it has been used in surface inception, health monitoring, infrastructure health monitoring, etc. In these applications, Ultra-wideband RADAR systems are more popular than traditional RADAR systems. Impulse RADAR is a special kind of ultra-wideband RADAR, which is mostly used for surface penetration, through-wall imaging, antimissile detection, anti-stealth technology, etc. because of its high resolution and low center frequency. Out of all these applications, impulse RADAR has been used intensively as a ground-penetrating RADAR for the detection of land mines, underlying pipelines, buried objects, etc. This report has attempted to provide the steps for designing the impulse ground penetrating RADAR (GPR) as well as provides the value of crucial parameters required in the design process of commercial GPR systems.**

***Keywords*—RADAR, Impulse RADAR, Ground Penetrating RADAR (GPR)**

I. Introduction

THE Impulse RADAR is a subset of Ultra-wideband (UWB) RADARs [1]. A UWB RADAR is one having a large relative bandwidth or fractional bandwidth where the fractional bandwidth is defined as the ratio between the absolute bandwidth and the carrier (or center) frequency (f_c). Mathematically it can be written as,

$$\eta_0 = \frac{\Delta f}{f_c} \qquad 0 \le \eta_0 \le 1 \qquad \text{where, } \Delta f = (f_H - f_L). \tag{1}$$

The conventional technology of RADAR is based on small relative bandwidth in the range 0.01<η0< 0.25, i.e., the absolute bandwidth is at most 25% of the carrier frequency whereas UWB RADAR is characterized by 0.25<η0< 1 [2]. Impulse RADAR being a particular case of UWB RADAR generates a single cycle sine wave. Such a signal would have a relative bandwidth of unity, i.e., a single-cycle sine wave has approximately 100 percent bandwidth, where percent bandwidth is defined as 100 times the absolute bandwidth divided by the carrier frequency, usual definition of an impulse RADAR [3]. The concept of impulse RADAR came into the picture in the early 1960s when John C. Cook proposed a single cycled VHF RADAR for measuring the thickness of the Ice [4]. In the late 1960s, the Impulse RADAR was studied by the US Department of defense as a method to explore the underground tunnels, buried objects, natural underground formations, etc. Ground probing remained the most attractive area of application for impulse RADAR for several years. Still, gradually, it has proved its importance in the field of Anti-Stealth technology, Anti-Missile Detection, Through-the-wall imaging, Sensor technology, etc.[1, 5], So, the essential requirement of an impulse RADAR is to have an absolute wide bandwidth. However, still, it's relative to carrier frequency because a conventional RADAR can have a large absolute bandwidth and always be narrow band. For example, a short pulse X-band (10 GHz) RADAR with 2 ns pulse width (500 MHz bandwidth) is narrowband as its bandwidth is small compared to the carrier frequency (5%). However, a 500 MHz bandwidth RADAR at UHF has a fractional bandwidth of 1 or 100% [3].The difference of characteristics between impulse RADAR and other wideband RADARs can be found out in its spectrum. The spectrum of a time-domain signal is given by its Fourier transform i.e.

$$s(f) = \int_{-\infty}^{\infty} s(t) * e^{-j2\pi ft}\, dt \tag{2}$$

Now putting $s(t)$ as a sine wave of duration τ and frequency f_0 in the above equation,

$$s(f) = \int_{-\frac{\tau}{2}}^{\frac{\tau}{2}} \sin(2\pi f_0 t) * e^{-j2\pi ft}\, dt$$
$$= \frac{j}{2\pi}\left[\frac{\sin(\pi(f_0+f)\tau)}{(f_0+f)} - \frac{\sin(\pi(f_0-f)\tau)}{(f_0-f)}\right] \tag{3}$$

When we consider that the sine signal contains exactly N cycles then the duration τ=N/f_0. Putting the value of τ in the above equation and calculating the magnitude of the spectrum as

$$|s(f)| = \frac{1}{\pi f_0}\left[\frac{sin\left(\frac{N\pi f}{f_0}\right)}{1-(f/f_0)^2}\right] \tag{4}$$

Putting N=1 for single cycle sine wave in the above equation, we will get the magnitude spectrum as

$$|s(f)| = \frac{1}{\pi f_0}\left[\frac{sin\left(\frac{\pi f}{f_0}\right)}{1-(f/f_0)^2}\right] \tag{5}$$

The bandwidth of a single cycle wave is exceptionally high, which makes it challenging to generate and radiate. In practice, due to the inability to achieve the required bandwidth, the

S. Kumar is with the Department of Electronics and Communication Engineering, Muzaffarpur Institute of Technology, Muzaffarpur, Bihar, India. (e-mail: sgsaket1@gmail.com).

A. Kumar is with the Department of Electronics and Communication Engineering, Bharati Vidyapeeth (Deemed to be University) College of Engineering, Pune, India (e-mail: amit.kumarc210@gmail.com).

V. Singh is with the Department of Electrical and Electronics Engineering, IIT Guwahati, India (e-mail: vs13@iitg.ernet.in).

A. K. Singh is with the School of Advanced Sciences, Department of Physics, Vellore Institute of Technology, Vellore, Tamil Naidu, India (e-mail: er. abhis.iitk@gmail.com).

waveform extends for more than one cycle in duration. However, it cannot be any number of cycles in span; otherwise, its bandwidth will no longer be wide enough, and it becomes more like a short-pulse RADAR.

A RADAR which generates Gaussian pulses with fractional bandwidth between 0.25 and 1 is also called as an impulse RADAR. Due to the high bandwidth of Gaussian pulses, they are suitable for UWB RADARs and even for impulse RADARs. Another property of a Gaussian pulse is that differentiating a Gaussian pulse provides a monocycle pulse. So, in many applications, the monocycle is generated by differentiating the Gaussian pulse [6]. In the rest of this paper, we are considering that both the monocycle as well as Gaussian pulse are being used in the impulse RADAR system. Another distinct property of impulse RADAR is the high transmitting power. Its peak power and average power characterize the transmitter of a RADAR. The shorter the pulse, the greater the peak power to have the same energy. For example, if a pulse of one microsecond has a peak power of one megawatt, the peak power in a 0.1 nanosecond pulse with the same energy must be 10 gigawatts. So the peak power of impulse RADARs must be higher than that of conventional RADARs to achieve the same energy on target. However, the average power and pulse energy of existing impulse RADARs are much lower than usually found in traditional RADARs, which is a good measure of the detection capability of a RADAR [3].

As mentioned earlier, impulse RADAR has been mostly used as ground probing RADAR, as given in the literature [2, 3, 7]. It has rarely been applied to some other applications till now. So my discussion on impulse RADAR is entirely in terms of GPR. However GPR has been used in various applications since 1960, until now it has not been widely commercialized. One of the reasons behind this is the lack of study of the variation of the properties of EM waves and various electronics used in the transmitter and receiver section when it comes in contact with the ground.

The rest of the paper is organized as follows. Section 2 includes the general introduction to GPR and the design process of GPR. Section 3 presents signal processing required in the receiver section. Section IV contains the specification of GPR systems available in literature as well as the specification of one commercially available GPR system, and Section V is the conclusion.

II. Ground Probing RADAR (GPR)

Ground probing refers to gathering information about the buried object in the earth's surface. It may refer to detecting the object or getting information about the composition of the object or knowing about the shape of the object. Application of the RADAR and characteristics of the RADAR in this scenario is different, but the basic principles of RADAR operation remain the same. A ground probing RADAR generates a monocycle signal and sends it into the ground from a dipole antenna with resistive loading. The most significant advantage of this type of RADAR is that the antennas need not touch the ground to send the signal. Then reflected signals are gathered by the same antenna as they are pulse RADARs, and it is processed to give suitable results to the operator.

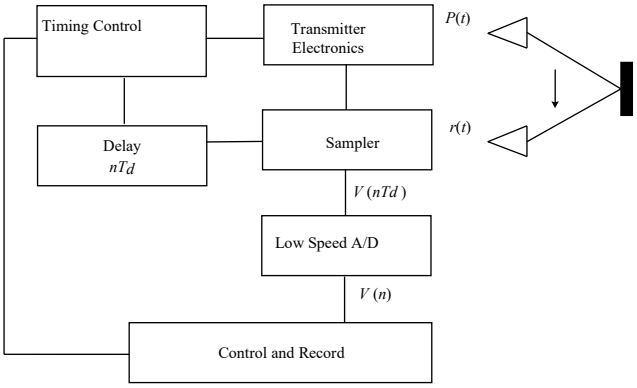

Fig. 1. Simplified system design for ground-penetrating RADAR [4].

For the ground-penetrating RADAR, the frequency of operation is selected by the properties of soil. The operating frequency is chosen below 1GHz. To achieve the excellent ground-penetrating capability, frequency should remain low because of the losses frequent in typical soil increase with the frequency [5]. This is the reason why the RADAR used for the ground probing purpose operates at low (<1GHz) center frequency but at very large bandwidth. The reason for high bandwidth is that the range resolution of a pulse RADAR is given as [6].

$$r_{res} = \frac{C}{2B} \tag{6}$$

Where r_{res} is the range resolution, C is the speed of light and B is the bandwidth of the pulse. So the higher the bandwidth, the higher the ability of the RADAR to separate two targets placed very close to each other. Due to the requirement of low center frequency and very high bandwidth, the choice of UWB RADAR becomes very obvious in this application. Many practical systems operate in the time domain and have a fractional bandwidth of approximately 100% [4], which refers to the impulse RADAR system.

The fundamental difference between the conventional RADAR and the RADAR used in surface penetration is that the traditional RADAR has a very long range of operation with coarse resolution. In contrast, the surface penetrating RADAR has a short-range with excellent resolution.

A. System Design Of A Ground Penetrating Radar

Fig.1 shows the basic block diagram of a GPR system. I3t consists of transmitter electronics (impulse generator), a timing circuit, a transmitting antenna, a receiving antenna, and a digitizing circuit. So, the design of a GPR system includes two parts. 1. Transmitter design 2. Receiver design. The transmitter

part consists of a pulse generator that generates a pulse which is fed to the antenna. So, the discussion of transmitter design includes pulse generator design and an Antenna design, which gets affected due to the various constraints on bandwidth, transmitter power, and center frequency. The receiver part comprises an antenna that senses the received signal and a sampler to capture the received signal.

B. TRANSMITTER DESIGN

The transmitter designing part can be grouped into four sections. The first part includes UWB pulse generation criteria; the second part contains the appropriate transmitter power selection criteria; the third part consists of the steps for center frequency selection for GPR, and the fourth part includes the antenna design and placing. All four sections are discussed one by one in the following subsections.

C. UWB PULSE GENERATION STRATEGY

There are three types of pulse waveforms: Gaussian-like, monocycle, and polycycle. The first two are more popular, and somehow the monocycle pulses are the most important in this field because of their more straightforward realization and broader spectrum [7]. So my discussion of pulse generation will be confined to Gaussian pulse generation and monocycle pulse generation.

Traditionally the UWB pulses or short duration pulses are generated by using the transmission line and some semiconductor devices, which can act as fast switches. Lee and Ngyuen in [11] provided the most basic method of UWB pulse generation, which uses a step recovery diode (SRD) and transmission line to generate a pulse. The use of SRD in switching circuits is widespread. The SRD acts as a common PN-diode when it is in forward bias. It stores charges in its depletion layer. But when the biasing abruptly changes to reverse bias, then suddenly SRD discharges and go to cut-off region sharply or suddenly, unlike other PN-diodes. This phenomenon makes it suitable for the generation of a very sharp step-like signal. So, the UWB generator mentioned in this paper uses a square pulse generator that is connected to the SRD, as shown in Fig.2.

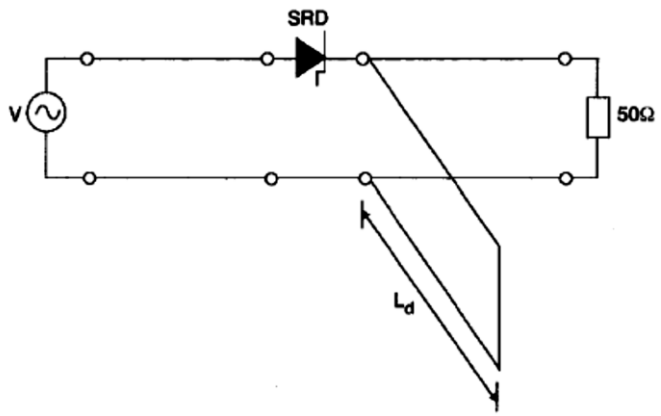

Fig.2. Gaussian pulse generation using an SRD and transmission line [11]

During the positive half of the square pulse, the SRD stores some charges, but when the pulse changes its polarity, suddenly SRD discharges and generates a very sharp step-like function. Now the given circuit has a main transmission line and a short-circuited stub. When the pulse reaches the junction, then it is divided into two directions. One goes towards the output port, and the other goes towards the short-circuited stub. As we know, the pulse is reflected back from the short-circuited path with reverse polarity, and it goes towards the output port with a delay. Now, both pulses will be added at the output, and they will generate a pulse of a short duration.

In the given figure, the pulse has a very sharp cut-off, which is practically impossible. So, it is a Gaussian pulse rather than a square pulse practically. Here the width of the pulse is $\boldsymbol{\tau}$which is the delay introduced by the short-circuited stub. So the pulse width depends on the stub length, which is given by (4).

$$\tau = \frac{2L_d}{v_p} \tag{7}$$

where $\boldsymbol{L_d}$ is the stub length and $\boldsymbol{V_p}$ is the phase velocity along with the stub. Hence, by only varying the length of the stub, we can control the duration of the pulse. In the year of 2004, another technique came into the picture where we can electronically tune the length of the transmission line to control

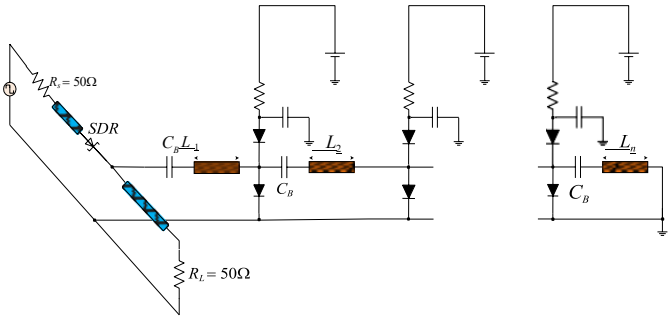

Fig. 3. Schematic of the PIN diode tuneable pulse generator [12]

the width of the pulse [12]. The circuit diagram for this tuneable pulse generator is given in Fig. 3.

This uses PIN diodes in the short-circuited stub in different positions $\boldsymbol{L_d}$ where ($\boldsymbol{d = 1, 2, \ldots . n}$). The biasing of PIN diodes is independent of each other. At a given time, one diode is forward biased, and all others are reverse biased, which provides the different length of short-circuited stub. It is reported that the pulses of width between 300ps and 800ps are generated by using this method. Here, the capacitors are used to block DC. Instead of a PIN diode, if we use MESFET, then there is no need for this capacitor. Hence, using MESFET provides more simplified and distortion less structure for pulse generation as that of the PIN diode. Another simple method to

generate the monocycle pulse from the Gaussian pulse is to differentiate the Gaussian pulse using the RC differentiator. Han and Nguyen in [9] used the same method with a Schottky diode to get the monocycle pulse. However, it is not tuneable like the method described above. Another technique that employs the UWB pulse generation by differentiating the Gaussian pulse is proposed in [10]. It takes the double derivative of the Gaussian pulse to generate a pulse of duration 800ps. Another method described in [11] uses SRD and a pulse shaping circuit for low ringing mono pulse generation. Nikoo and Hashemi [11] proposed a new way of generating a very narrow width pulse of duration 1ns. It uses an SRD, two coupled diodes, a high current diode, and a gate discharge tube. It provides an output power level of 5.7 MW with a repetition frequency of 450 KHz.

The above two methods were used for the generation of Gaussian pulse. Slightly modifying the circuit can generate a monocycle pulse. The basic principle for the generation of monocycle pulse is that after generating the Gaussian pulse, again transmit that pulse through a short-circuited transmission line to produce the same pulse with reverse polarity. Then by adding both the pulses with some delay, we can get a monocycle pulse. The tuneable monocycle pulse generation is described in [6]. Fig.4 shows that the Gaussian pulse generating circuit is attached to the tuneable pulse generating circuit shown in Fig. 3 to form a monocycle pulse generator.

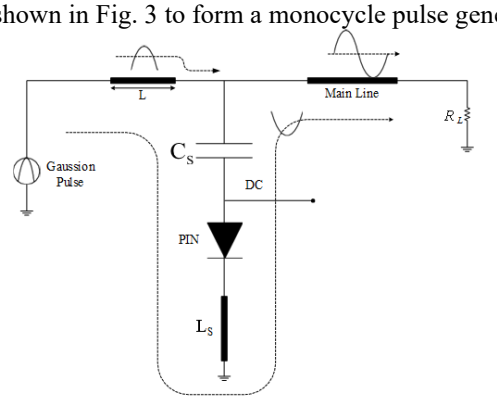

Fig.4. Schematic of a monocycle pulse generator [6]

Another method that uses MESFET to generate a monocycle pulse is described in [7]. Here the MESFET provides a better impedance matching between the Gaussian pulse generator and monocycle pulse generator. Although all these methods offer a short duration Gaussian pulse, as they use the devices like SRD, it is challenging to integrate them into standard CMOS circuits.

Recently, many methods have been proposed for the design of UWB pulse generators, which can be integrated into digital CMOS for low cost and reconfigurable pulse shape. A simple way to start with is considering baseband pulse with the low-pass spectrum and then up-convert it to the target frequency band. This method includes a baseband pulse generator, a local oscillator, and a multiplier. The local oscillator controls the desired frequency band. We can fix the oscillating frequency, or we can make it voltage-dependent. Fig.5 shows the schematic for this method. Cavallaro et al. [13] designed a UWB pulse generator based on this technique in 90 nm CMOS. The carrier frequency is set in between 3.5 GHz and 4.5 GHz in steps of 500 MHz. This type of method is otherwise called as the heterodyning method or carrier-based approach for the UWB pulse generation.

Another method for UWB pulse generation in CMOS technology is called analogue filtering [14], where we generate an impulse in the time domain and use a pulse-shaping filter. The UWB pulse center frequency and bandwidth entirely depend on the pulse shaping filter used.

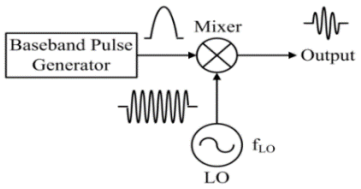

Fig. 5. UWB pulse generation by Heterodyning Method

S. Bourdel et al. [15] proposed a method to generate an impulse in the time domain by digital logic circuit then use a third-order ladder Bessel filter as a pulse-shaping filter. A digital logic circuit is given in Fig. 6 to generate impulses, where it includes an inverter and a NOR gate for impulse generation. NOR gate can be replaced by the NAND gate to generate impulse of opposite polarity. The sole purpose of the inverter is to introduce a small delay to the trigger signal. In this paper, it implements a high-speed current mode logic (CML) to generate a pulse of duration 75ps. Table I summarizes all the UWB pulse generation methods available in the literature.

TABLE I

All the pulse generation methods in a compact form

Ref.	Technology involved	Specifications
[7]	MESFET and transmission line	300-ps monocycle pulses with about 2 V peak-to-peak and a pulse repetition rate of 10 MHz
[8]	Step recovery diode and transmission line.	154 ps pulse width, 3.5 v amplitude
[9]	PIN diode, MESFET, Transmission line	300 to 800 ps pulse width
[10]	Schottky diode and transmission line.	300 ps pulse width with -17dB ringing level
[11]	Step recovery diode and transmission line	800 ps pulse width
[12]	Step recovery diode, gate discharge tube	1ns pulse width with 5.7 Mw of output power
[13]	Carrier based UWB generation, CMOS	1.5-2.5 ns pulse width
[14]	Digital logic circuit	75 ps pulse width
[15]	Avalanche transistor	2 ns pulse width
[16]	FPGA base GPU	1ns narrow pulse width for Ultrawideband technology
[17]	0.18 µm CMOS technology	peak-to-peak amplitude of the pulse is 673 mv and the duration is 500ps.
[18]	A nanosecond pulse generator based on Avalanche transistor	900 ps pulse width and an amplitude of 25.2V
[19]	Compact step recovery diode sub nanosecond pulse generator	amplitude of this pulse reaches 7.5 V, and the pulse has an Full-Width at Half-Maximum of about 110 ps

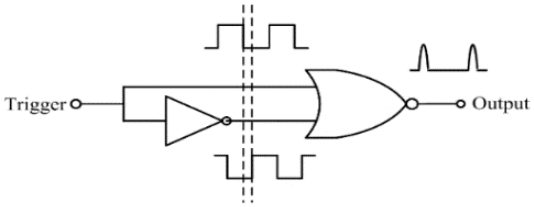

Fig. 6. Digital logic circuit for impulse generation

D. TRANSMITTER POWER CALCULATION

As it is mentioned before, GPR has a short-range because the EM wave has to travel through a lossy medium known as ground. RADAR range equation is given

$$P_r = \frac{P_t G^2 \sigma (\lambda / \in_r)^2}{(4\pi)^2 R^4 L} \tag{8}$$

where $\boldsymbol{P_r}$ is the total received power, $\boldsymbol{P_t}$ is the total transmitted power,$\boldsymbol{R}$ is the range of the RADAR and the most crucial term here in this equation is $\boldsymbol{L}$ which is termed as the loss component. So, the range of the RADAR depends on the loss component, which itself depends on the wavelength (λ) of operation, target size, the conductivity of the target (σ), property of the ground, etc. The critical parameter in the designing of a GPR is that the user must define the depth of penetration for the RADAR. We need to calculate the required center frequency, power to be launched, and required bandwidth depending on our necessary penetration depth as well as resolution. If we fix the range, then we can get our power requirement. As has been shown in the RADAR range equation, the power required for the RADAR is clearly dependent on the losses that occur during the propagation of the wave from the source to the target and vice versa, all the losses that limit the performance of a GPR are discussed. Total losses can be written as:

$$L_T = L_e + L_m + L_{t1} + L_{t2} + L_s + L_a + L_{sc} \tag{9}$$

Where, L_T = total path loss for a given distance in dB

L_e = antenna efficiency loss in dB

L_m = antenna mismatch loss in dB

L_{t1} = transmission loss from air to material in dB

L_{t2} = transmission loss from material to air in dB

L_s = antenna spreading loss in dB

L_a = attenuation loss of material in dB

L_{sc} = target scattering loss in dB

a. ANTENNA EFFICIENCY LOSS

Antenna efficiency is defined as what fraction of the power can be radiated from the total power supplied to the antenna terminal. For the impulse GPR, we need a wideband antenna. Generally, the dipole antenna is converted to a wideband dipole antenna by resistive loading [21]. However, due to the resistive loading, efficiency decreases [21]. The typical efficiency of resistive loaded dipole antenna is around 4dB in 100MHz of frequency.

b. ANTENNA MISMATCH LOSS

Mismatch occurs when there is an impedance mismatch between the transmitter and antenna. There is always a mismatch between them due to which there is a small power loss, which is called antenna mismatch loss.

c. TRANSMISSION LOSS FROM AIR TO MATERIAL

As the ground-penetrating RADAR works on the surface, so there is a loss when an electromagnetic wave travels from air to the material or ground. The loss due to this is called the coupling loss between two media. This can be calculated as [22] (10).

$$L_{t1} = -20\log\left(\frac{4 z_m z_a)}{|z_m + z_a|^2)}\right) \text{ dB} \tag{10}$$

Here Z_a is the characteristic impedance of the air (377 ohms)

Z_m is the characteristic impedance of the material, and it can be written as where all the symbols carry their usual meaning.

$$z_m = \left(\sqrt{\frac{\mu_r \mu_0}{\in_r \in_0}}\right)\left(\frac{1}{\left(1+(\tan\delta)^2\right)^{1/4}}\right)\left(\cos\frac{\delta}{2} + j\sin\frac{\delta}{2}\right) \tag{11}$$

E. TRANSMISSION LOSS FROM MATERIAL TO AIR

This coupling loss is encountered when the reflected signal comes from ground to the air medium. It can be calculated as [22]:

$$L_{t2} = -20\log\left(\frac{4 z_m z_a)}{|z_m + z_a|^2)}\right) \text{ dB} \tag{12}$$

a. SPREADING LOSS

This loss occurs for every point source. When the signal propagates, the power decreases rapidly with respect to distance, and the loss is given as [25]:

$$L_s = -10\log\left(\frac{G_t A \sigma}{(4\pi R^2)^2}\right) \text{ dB} \tag{13}$$

Here G_t is the transmitting antenna gain. A is the aperture area of the antenna. σ is the RADAR cross-section while R is the distance between the target and the source. Here, the formula above is given for a point reflector. But depending on the type of reflector, the received power varies. For the case of line reflector like pipeline beneath the ground, the scattering loss is inversely proportional to the R^{-3} [22]. So, depending on the target, we can estimate our transmitted power and received power.

b. TARGET SCATTERING LOSS

Target scattering loss can be expressed as [22]:

$$L_{sc} = 20\log\left(1-\frac{Z_1-Z_2}{Z_1+Z_2}\right)+20\log\sigma \text{ dB} \quad (14)$$

Z_1 - The characteristic impedance of the first layer of material

Z_2 - The characteristic impedance of the second layer of material

σ - RADAR cross-section

This L_{sc} varies according to the geometry of the scatterer, type of the material, whether metal or non-metal.

c. MATERIAL ABSORPTION LOSS

Material absorption loss can be expressed as [22]:

$$L_a = 8.686 * R * 2\Pi f \sqrt{\left(\frac{\mu_0\mu_r\in_0\in_r}{2}\left(\sqrt{1+\left(\tan\delta\right)^2}\right)-1\right)} \quad (15)$$

The material absorption loss is dependent on the frequency.

After calculating all the losses and knowing the transmitted power or voltage, we can calculate the received or reflected power from the target. If transmitted power is p_t and the received power is p_r then the detectability of the receiver is given as [22]:

$$D = 10\log\left(\frac{p_t}{p_r}\right) \quad (16)$$

If the detectability is above the noise level of the receiver, then we can detect the target and can process it further. This detectability parameter is used in all the literature that concentrates on system design [23, 24, 25]. All these losses are included in the spreadsheet for the analysis of the RADAR range before the actual design of the RADAR.

d. CALCULATION OF CENTER FREQUENCY

From the above discussion, we can get the knowledge about the range of the RADAR with given input power and detectability of the receiver or vice versa. Again, the depth of penetration depends on the frequency of operation. So, as the frequency increases, losses also increase. So, one can say that the lower is the frequency, the more be the depth of penetration. However, another factor that affects the depth of penetration is the resolution of the RADAR. As we can see from (1), the resolution of the RADAR directly depends on the frequency. More be the frequency better be the resolution. When there are multiple features to be detected like the detection of buried pipes and cables, then receiver bandwidth should be more for resolving the targets successfully. So GPRs have to compromise between depth of penetration and the resolution. Another factor that affects the frequency selection process is clutter. The clutter comes into the picture because when the EM waves propagate into the soil, some parts of it get scattered due to the heterogeneity of the host material. This scattered signal is not related to the message we intend, and it is called as clutter. Another reason for the clutter is that when the transmitter transmits the EM waves, some parts of it get transferred to the receiver. Experimentally it has been shown that clutter increases as the frequency increases. So if the operating frequency is very large, then we can't separate our signal coming from the target concerning clutter signal. Considering all these facts, the calculation of center frequency for GPR is the key to its applicability for a particular application.

For the calculation of center frequency, we have to compromise between three things,

1) Spatial resolution
2) Clutter limitation
3) Exploration depth

Each of these three events put restrictions on the selection of the center frequency. We have to discuss how these three requirements affect our frequency selection. Assuming the ratio between center frequency and bandwidth be one, the restriction on the center frequency due to the spatial resolution can be expressed as [25]:

$$f_c^R > \frac{75}{\Delta z\sqrt{K}}\,MHz \quad (17)$$

Here Δz is the distance between the two targets, which are to be distinguished from one another, and it is expressed in terms of meters. 'K' is the dielectric constant or relative permittivity.

To achieve a greater depth of penetration, the clutter should be minimized as much as possible. So to accomplish this, the wavelength that we use should be higher than that of the clutter dimension. A typical value is, the wavelength is 10 times greater than the clutter dimension (Δl). So the restriction on the center frequency due to the clutter can be expressed as [25]:

$$f_c^C < \frac{30}{\Delta l\sqrt{K}}\,MHz \quad (18)$$

It is always desirable that the significant part of the target should fall into most of the part of the RADAR beam so that most of the energy will be reflected back. So target size should be nearer to the Fresnel zone size. These affect the selection of center frequency, and it affects the depth of penetration. So restriction can be mathematically written as [25]:

$$f_c^D < \frac{v\beta\sqrt{K-1}}{D}\,MHz \quad (19)$$

Here β is the ratio between target size and RADAR footprint. For GPR, the value β is typically 4 [25]. Finally, the center frequency is calculated by following the rule given below.

$$f_c^R < f_c < \min\left(f_c^C, f_c^D\right) \quad (20)$$

The essential factor that plays a significant role in determining center frequency is the dielectric constant or relative permittivity of the medium. Table II contains the dielectric constant and attenuation of the different mediums.

Once we decide the center frequency, then bandwidth can be calculated in such a way that the ratio between them should

approach 1. If the resolution frequency is more than that of the other two frequencies, then that resolution can't be supported in the RADAR system. Another beneficial relation and one of the fundamental relationships is that [25]:

$$BW = \frac{1}{Pulsewidth} \tag{21}$$

With the above expression, the complete discussion on the selection of BW, center frequency, pulse width, and transmitter power has come to an end.

The receiver designing part can be grouped into three parts. The first part includes designing the receiving antenna; the second part consists of the appropriate sampler circuit selection; the third part provides signal processing required to improve SNR.

III. Signal Processing at the Receiver

A. Receiver Bandwidth Calculation

Receiver bandwidth is calculated by calculating the power spectral density of the received signal. However, we can model this whole procedure and calculate the receiver bandwidth beforehand. If we consider the transmitted pulse is of Gaussian shape, then the target reflected signal can be modeled as the fourth derivative of the Gaussian pulse [26].

Table II
List of specifications of GPR systems available in literature

Ref.	Purpose	Specifications
[27]	Detecting small metal objects in the Ground	-Operating frequency-100-400MHz, Antenna-Broadband dipole antenna with 100MHz to 350MHz -Sampling interval- 100ns PRF-10KHz, The separation between the antenna-0.8m
[28]	Surface probing, Pavement probing	-Frequency of operation-100MHz to 1GHz, The center frequency of Antenna- 100 MHz -PRF-300 KHz, Sampling interval- 0.1ns, Antenna- Horn antenna with loading.
[29]	GPR system that could penetrate to tens of meters with 1-2 m resolution.	-Centre frequency-50MHz,100MHz, System Performance-155Db -Sampling Interval-800ps, Antenna frequency-100MHz
[30]	Nondestructive Evaluation of Pavements Integrated chip for GPR	-Pulse width- 330ps, Sampling rate of receiver-(0-6)GHz -Antenna operating, frequency- (0.2-20)GHz

Both modeled received signal and experimental signal are shown in Fig. 7. Again the ground can be modeled as a low pass filter, which causes pulse broadening in the received signal [26]. So, as compared to the transmitted signal, the received signal spreads due to electrical properties and attenuation in the ground. If the attenuation is more, then the spreading is more. Fig. 7 shows the transmitted and received pulse.

An estimate of this spread can be calculated from the model depending on the soil characteristics [24] and so as receiver bandwidth from received pulse width by using the relation

$$BW = \frac{1}{Pulsewidth} \tag{22}$$

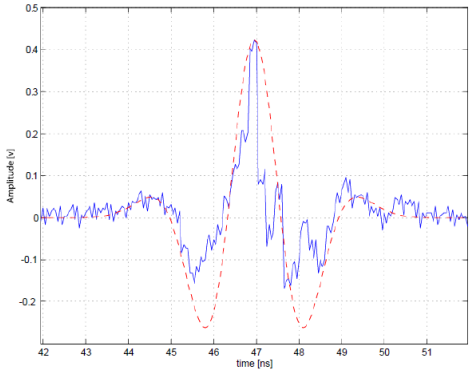

Fig. 7. Modeled received signal (dotted) and experimental received signal of 4-Channel Bidirectional Audio A/D & D/A Converter (ADA4) [26]

B. Receiver Noise Figure Calculation

The noise figure calculation is described as an example. In [26], the Tektronix oscilloscope acts as receiver and detector in the prototype GPR system. So depending on its specification, the noise figure is calculated. It employs an 8-bit digitizer. Sensitivity is 2mv/division. So the total deflection is 16mv. Again the resolution of the ADC is 4.8 bits. So 3bits are lost due to noise. The bandwidth of the receiver is 4GHz.

Depending on these values, the noise figure is calculated as follows. As full-scale deflection is 16mv, so 16mv is available for 256 levels. Per level, the voltage is 0.0625mv. As we know, 3bits are lost due to noise, so the output noise signal is 0.0625*8= 0.5 mv. The input signal is obtained from thermal noise and calculated using the expression

$$v_{rms}^2 = 4KTBR \tag{23}$$

Where, K-Boltzmann Constant, T-Operating temperature (300K), B-Receiver bandwidth, R-Characteristics resistance. Putting all the values, the input noise power is calculated as $3.3 \times 10^{-9} V^2$.

Finally, $NF = \frac{outputNP}{InputNP}$=19dB (24)

IV. GPR Systems Available in Literature:

Few GPR systems that are reported in the literature are listed in Table II. The detailed specification of a RADAR system is also mentioned.

V. Conclusion

In this paper, the introduction to impulse RADAR, the connection between impulse RADAR and Ground probing RADAR, steps for the transmitter, and receiver design of a ground-penetrating RADAR along with signal processing required at the receiver have been discussed. All the available

literature lack this feature in their content. Summarizing the shortcomings present in literature in steps are:

1) Very few papers are available, which contains the complete design of an impulse GPR prototype.
2) Sufficient literature is not available on the complete design process of GPR. As an, e.g., some papers have concentrated on the pulse generation method, whereas others focused only on designing the antenna for GPR systems.
3) Commercially available GPRs have classified specifications.

In this review report, we tried to bring the whole design procedure together in a single report. Summarizing the entire design procedure of the GPR RADAR, it consists of mainly two steps. 1. Transmitter design 2. Receiver design. Transmitter design steps can be briefly written in 4 steps.

1) Define the depth of penetration of the RADAR.
2) Given the dielectric constant of the host material the center frequency and bandwidth is calculated as given in section E.
3) Given the frequency of operation, depth of penetration,
4) And the detectability of the receiver, the transmitted power is calculated as provided in section D.
5) Depending on the bandwidth and the frequency of operation, the pulse width is chosen, and an appropriate pulse generation strategy is applied as given in section C along with the selection of proper antenna, antenna orientation, and antenna spacing for transmitting this pulse.

The receiver design can be summarized in 3 steps.

1) Receiver Antenna selection is the same as that of a transmitter
2) The receiver sampling circuit and ADC is selected as that of section G.
3) Receiver bandwidth, Noise figure calculation along with required signal processing is done according to section III.

This report doesn't deal with the procedure of data interpretation from the GPR scan. As a future scope, we are going to design an impulse RADAR for a specific ground probing application so that a detailed calculation of all the parameters can be done. As the designing procedure strictly depends on the properties of the host material, target properties, so before designing the RADAR, a detailed survey of the corresponding geographical area is required.

REFERENCES

[1] M.G.M. Hussain, "Ultra-wideband impulse RADAR-An overview of the principles," *IEEE Aerosp. Electron. Syst. Mag.*, vol. 13, no. 9, pp. 9 -14, 1998. DOI: https://doi.org/10.1109/62.715515.

[2] D. L. Black, "An overview of impulse RADAR phenomenon," *IEEE AES Systems Magazine*, pp. 6-11, Dec. 292. DOI: https://doi.org/10.1109/NAECON.1992.220600.

[3] M. I. Skolnik, "An Introduction To Impulse RADAR", 1990.

[4] D. Daniels, "Applications of impulse RADAR technology," *Proc. RADAR Systems (RADAR 97)*, pp. 667 -672. DOI: https://doi.org/10.1049/cp:19971759.

[5] M. Sato, "Principles of mine detection by ground-penetrating RADAR,"*Anti-personnel Landmine Detection for Humanitarian Demining*, Springer London, 2009. 19-26. DOI: https://doi.org/10.1007/978-1-84882-346-4_2.

[6] M. N. Cohen, "An overview of high range resolution radar techniques," *NTC '91 - National Telesystems Conference Proceedings*, Atlanta, GA, USA, 1991, pp. 107-115, DOI: https://doi.org/10.1109/NTC.1991.147997.

[7] J. S. Lee and C. Nguyen, "Novel low-cost ultra-wideband, ultra-short-pulse transmitter with MESFET impulse-shaping circuitry for reduced distortion and improved pulse repetition rate," *IEEE Microwave Wireless Compon. Lett.* , vol.11, pp. 208 -210, 2001. DOI: https://doi.org/10.1109/7260.923030.

[8] J. S. Lee and C. Nguyen, "Uniplanar picosecond pulse generator using step-recovery diode," *Electron. Lett.,* vol. 37, pp. 504–506, 2001. DOI: https://doi.org/10.1049/el:20010350

[9] J. Han and C. Nguyen, "Ultra-wideband electronically tuneable pulse generators," *IEEE Microw. Wireless Compon. Lett.*, vol. 14, no. 3, pp. 112 -114, 2004. DOI: https://doi.org/10.1109/LMWC.2004.825184.

[10] J. Han and C. Nguyen, "A new ultra-wideband, ultra-short monocycle pulse generator with reduced ringing," *IEEE Microwave Wireless Compon. Lett.*, vol. 12, pp. 206 -208, 2002. DOI: https://doi.org/10.1109/LMWC.2002.1009996.

[11] Yan Xiao, Zhong-Yong Wang, Li, J., Zi-Lun Yuan , "Design of a Second-Derivative Gaussian pulse generator," *IEEE International Conference on Signal Processing, Communication and Computing (ICSPCC),* pp. 1 – 4, 2013. DOI: https://doi.org/10.1109/ICSPCC.2013.6663994.

[12] M.S. Nikoo, S.M.A. Hashemi., "High-Power Nanosecond Pulse Generator With High-Voltage SRD and GDT Switch," *IEEE Trans. Plasma Sci.* ,vol. 43, no. 9, pp. 3268-3276, Sept. 2015. DOI: https://doi.org/10.1109/TPS.2015.2411251.

[13] M. Cavallaro, E. Ragonese and G. Palmisano, "An ultra-wideband transmitter based on a new pulse generator," *Proc. IEEE Radio Freq. Integ. Circuits Symp*, pp. 43-46, 2008. DOI: https://doi.org/10.1109/RFIC.2008.4561382.

[14] El-Gabaly, "Pulsed RF Circuits for Ultra Wideband Communications and RADAR Applications," Ph.D dissertation, Dept. Elect. Comput. Eng., Queen's University, Canada, Aug. 2011.

[15] S. Bourdel et. al., "A 9-Pj/Pulse 1.42-Vpp OOK CMOS UWB pulse generator for the 3.1-10.6-GHz FCC band," *IEEE Trans. Microw. Theory Tech.*, vol. 58, no. 1, pp. 65, 2010. DOI: https://doi.org/10.1109/TMTT.2009.2035959.

[16] Aitykul Omurzakov, Ahmet K. Keskin., "Avalanche Transistor Short Pulse Generator Trials for GPR," *2016 8th International Conference on Ultra wideband and Ultra short Impulse Signals)*, Dec. 2016. DOI: https://doi.org/10.1109/UWBUSIS.2016.7724188.

[17] Ran Zhang, Lai-Liang Song., "Research on narrow pulse generation for ultra-wideband communication," *2016 13th International Computer Conference on Wavelet Active Media Technology and Information Processing (ICCWAMTIP)*, Dec. 2016. DOI: https://doi.org/10.1109/ICCWAMTIP.2016.8079860.

[18] S. Sim, D. Kim and S. Hong, "A CMOS UWB Pulse Generator for 6–10 GHz Applications," *IEEE Microwave and Wireless Components Letters*, vol. 19, no. 2, pp. 83-85, Feb. 2009, DOI: https://doi.org/10.1109/LMWC.2008.2011318.

[19] K. Zhou, C. L. Huang and M. Lu, "A nanosecond pulse generator based on avalanche transistor," *2016 16th International Conference on Ground Penetrating Radar (GPR)*, Hong Kong, 2016, pp. 1-5, DOI: https://doi.org/10.1109/ICGPR.2016.7572649.

[20] P. Protiva, J. Mrkvica, and J. Macháč, "A compact step recovery diode subnanosecond pulse generator," Microw. Opt. Technol. Lett., 52: 438-440. DOI: https://doi.org/10.1002/mop.24945 .

[21] T.P. Montoya, G.S. Smith, "A study of pulse radiation from several broad-band loaded monopoles," *IEEE Trans. Antennas Propag.*, vol. 44, no. 8, pp. 1172-1182, Aug 1996. DOI: https://doi.org/10.1109/8.511827.

[22] David J. Daniels, *Ground Penetrating RADAR*, 2nd Edition, IET, 2005. DOI: https://doi.org/10.1049/PBRA015E.

[23] S. Vitebskiy, L. Carin, M. A. Ressler and F. H. Le, "Ultra-wideband, short-pulse ground-penetrating radar: simulation and measurement," *IEEE*

Transactions on Geoscience and Remote Sensing, vol. 35, no. 3, pp. 762-772, May 1997, DOI: https://doi.org/10.1109/36.581999.

[24] M.A. Gonzalez-Huici, U. Uschkerat, V. Seidel, C. Pedlow, "A preliminary study of the radiation characteristic of an experimental GPR antenna for underground cavity detection," *IEEE International Conference on Microwaves, Communications, Antennas and Electronics Systems (COMCAS),* 2011, pp. 1-5, 7-9 Nov 2011. DOI: https://doi.org/10.1109/COMCAS.2011.6105908.

[25] A .P.Annan, *Ground Penetrating RADAR Principles, Procedures & Applications*, 2003.

[26] Greg Barrie, "UWB Impulse RADAR Characterization and Processing Techniques," *Defence R&D Canada, Ottawa, Tech. Rep. TR* 2004-251, Dec. 2004.

[27] Y.J. Park et al., "Development of a UWB GPR System for Detecting Small Objects Buried under Ground," *IEEE Conf. on ultra-wideband systems and Technologies,* 2003, pp.384-388. DOI: https://doi.org/10.1109/UWBST.2003.1267869.

[28] M. Yan, M. Tian, L. Gan and X. Chen, "Impulse Ground Penetrating Radar Hardware System Design," *2006 6th International Conference on ITS Telecommunications*, Chengdu, 2006, pp. 1244-1247, DOI: https://doi.org/10.1109/ITST.2006.288852.

[29] A.P. Annan, L.T. Chua, "Ground penetrating RADAR performance predictions," *Ground penetrating RADAR, ed. J. Pilon; Geological Survey of Canada,* Paper 90-4, pp. 5-13*,* 1992.

[30] Jeong Soo Lee, Cam Nguyen and T. Scullion, "A novel, compact, low-cost, impulse ground-penetrating radar for nondestructive evaluation of pavements," *IEEE Transactions on Instrumentation and Measurement*, vol. 53, no. 6, pp. 1502-1509, Dec. 2004, DOI: https://doi.org/10.1109/TIM.2004.82730.